Am J Cancer Res 2014;4(6):764-775
www.ajcr.us /ISSN:2156-6976/ajcr0002399

Original Article

Inhibition of mTOR reduce Stat3 and PAI related angiogenesis in salivary gland adenoid cystic carcinoma

Guang-Tao Yu[1,2*], Lin-Lin Bu[1,2*], Yu-Yue Zhao[1], Bing Liu[1], Wen-Feng Zhang[2], Yi-Fang Zhao[1,2], Lu Zhang[1], Zhi-Jun Sun[1,2]

[1]The State Key Laboratory Breeding Base of Basic Science of Stomatology & Key Laboratory of Oral Biomedicine Ministry of Education, [2]Department of Oral and Maxillofacial-Head and Neck Oncology, School and Hospital of Stomatology, Wuhan University, Wuhan, 430079, China. [*]Co-first authors.

Received September 9, 2014; Accepted September 24, 2014; Epub November 19, 2014; Published November 30, 2014

Abstract: Angiogenesis is a complex biological process, which is involved in tumorigenesis and progression. However, the molecular mechanism of underlying angiogenesis remains largely unknown. In this study, we accessed the expression of proteins related angiogenesis by immunohistochemical staining of human tissue microarray which contains 72 adenoid cystic carcinoma (AdCC), 12 pleomorphic adenoma (PMA) and 18 normal salivary gland (NSG) using digital pathological scanner and scoring system. We found that the expression of p-S6$^{S235/236}$ (a downstream molecule of mTOR), p-Stat3^{T705}, PAI, EGFR, and HIF-1α was significantly increased in AdCC as compared with PMA and (or) NSG ($p < 0.05$). While, the expression of these proteins was not associated with pathological type of human AdCC ($p > 0.05$). Correlation analysis of these proteins revealed that p-S6$^{S235/236}$ up-regulates the expression of EGFR/p-Stat3^{T705} ($p < 0.05$) and HIF-1α/PAI ($p < 0.05$). Moreover, the activation of p-S6$^{S235/236}$, EGFR/p-Stat3^{T705} and HIF-1α/PAI associated with angiogenesis (CD34) and proliferation (Ki-67). In vitro, Rapamycin suppressed the expression of p-S6$^{S235/236}$, EGFR, p-Stat3^{T705}, HIF-1α and PAI. Further more, target inhibition of mTOR by rapamycin effectively reduced tumor growth of SACC-83 cells line nude mice xenograft and decreased the expression of p-S6$^{S235/236}$, EGFR/p-Stat3^{T705} and HIF-1α/PAI. Taken together, these data revealed that mTOR signaling pathway regulates tumor angiogenesis by EGFR/p-Stat3^{T705} and HIF-1α/PAI. Inhibition of mTOR by rapamycin could effectively reduced tumor growth. It is likely that mTOR inhibitors may be a potential candidate for treatment of AdCC.

Keywords: Adenoid cystic carcinoma, angiogenesis, mTOR, Stat3, PAI, rapamycin

Introduction

Adenoid cystic carcinoma (AdCC), a common malignant tumor of salivary glands [1, 2], is generally characterized by unpredictable growth, extensive perineural invasion, and high rates of metastasis and recurrence [3]. The treatment of AdCC includes surgical resection, followed by radiation and (or) chemothreapy. Despite this regressive treatment, no significant improvement has been obtained for overall survival in the last three decades [4]. AdCCs are rather rare malignancy with quite different molecular pathology as compared with head neck squamous cell carcinoma. There is an urgently need to explore the molecular mechanism and novel drug target for AdCC. Of interest, among the network molecular mechanism dysregulated in AdCC, emerging basic, preclinical and clinical findings support the importance of mammalian target of rapamycin (mTOR) mediated cell proliferation, invasion, autophagy and apoptosis evasion [5-9]. Activation of mTOR phosphorylates S6K1 kinase (a eukaryotic translation regulator) [10]. The activation of S6K1 kinase phosphorylate substrate S6 to regulate a subset of mRNA translation in response to a wide variety of environmental signals, resulting in tumor angiogenesis and proliferation [11]. Indeed, previous studies consistently confirm that a high expression of p-S6 is associated with angiogenesis, autophagy and apoptosis evasion of AdCC [7-9]. However, the mechanism underlying the effect of p-S6 on the signaling transduction pathway which is activated in AdCC remains unclear.

Signal transducer and activator of transcription (Stat) constitute a family of cytoplasmic transcription proteins, including Stat1, Stat2, Stat3,

Stat4, Stat5A, Stat5B and Stat6 [12]. Stat3, gene has been mapped to chromosome 12 [13], was activated by phosphorylation in response to extracellular ligands such as cytokines and growth factors [14]. As far as we know, Stat3 was expressed and activated in a variety of primary tumors, including breast cancer [15], lung cance [16] and head and neck squamous cell carcinoma [17]. Moreover, activation and phosphorylation of EGFR can promote Stat3 phosphorylation [18]. However, the correlations among p-S6, EGFR and Stat3 have remained unclear in human AdCC.

Plasminogen activator inhibitor (PAI) is a serine protease inhibitor family, decreasing plasmin generation and fibrinolytic potential by covalently binding to tissue-type plasminogen activator (tPA) and urokinase-type plasminogen activator (uPA) [19]. Mice xenograft experiment indicated that inhibition of PAI can decrease tumor angiogenesis [20]. Recently, hypoxia-inducible factor-1α (HIF-1α) mediates TGF-β induced PAI production has been described in addition to its classic role in fibrinolysis inhibition [21, 22].

Based upon the above concerns, we hypothesize that mTOR induced p-S6$^{S235/236}$ regulates tumor angiogenesis depend on EGFR/p-Stat3^{T705}, HIF-1α/PAI signaling pathway. In this paper, we detected the expression of p-S6$^{S235/236}$, EGFR, p-Stat3^{T705}, HIF-1α and PAI using human tissue microarray. Correlation of these proteins with angiogenesis (CD34) and proliferation (Ki67) were analyzed in human AdCC. Furthermore, we investigated the effect of target inhibition of mTOR by rapamycin in vitro and vivo.

Materials and methods

Chemical and reagents

All chemical and reagents were purchased from Sigma-Aldrich unless specified. Rapamycin was purchased from LC Laboratory (Woburn,MA), Primary antibody against human p-S6$^{S235/236}$, EGFR, p-Stat3^{T705}, HIF-1α, Ki-67 were purchased form Cell Signaling Technology (Danvers, MA). Primary antibody against PAI was purchased form Proteintech Inc. (Chichago, IL) and CD34 was purchased from BD Pharmingen (San Diego, CA).

Ethics statement

This study was approved by the Medical Ethics Committee of Hospital of Stomatology Wuhan University (PI: Zhi-Jun Sun) and was performed according to the Institutional Guidelines. Written informed consent was obtained from participants. Animal studies were approved and supervised by the Laboratory Animal Care and Use Committee of Wuhan University.

Patient samples and tissue microarray

All tissue samples were obtained from AdCC and PMA patients surgically treated in the department of Oral and Maxillofacial Surgery, School and Hospital of Stomatology Wuhan University using formalin-fixed, paraffin-embedded (FFPE). For tissue microarray (T12-412-TMA1), we constructed a cohort including 72 AdCC (cribriform pattern: 28, tubular pattern 24, solid pattern 20, 50 patient overlap with previous described [9]), 12 PMA and 18 NSG in collaboration with Shanghai Biochip Company, Ltd, Shanghai, China (PI: Zhi-Jun Sun). All tumors were histology analyzed and classified according to the 2005 World Health Organization classification system [23].

Cell culture, nude mice xenografts and rapamycin treatment

SACC-83 cell lines of human salivary ACC were obtained from the China Center for Type Culture Collection, and were grown in Dulbecco's modified Eagle's medium (DMEM) supplemented with 10% FBS. The cells were incubated in a humidified atmosphere of 95% air and 5% CO_2 at 37°C. All animal experiments presented in our study were conducted according to the National Centre for the Replacement Refinement & Reduction of Animals in Research specified in protocols approved by the Laboratory Animal Care and Use Committee of Wuhan University. All animal procedures were performed under anaesthesia by 4% chloral hydrate and all efforts were made to decrease suffering. In our study, Female BALB/c nude mice (18-20 g; 6-8 weeks old) were purchased from Experimental Animal Laboratory of Wuhan University. Mice were housed in appropriate sterile filter-capped laminar flow cabinets under specific pathogen-free condition, fed and watered ad libitum with 12 h bright and 12 h

dark. SACC-83 cells (2×10^6 in 0.2 ml of medium) were inoculated subcutaneously into the flank of the mice. When the tumors reached a palpable size after 10 days, mice were randomly divided into a control group (n = 5 mice) or a group that received 10 mg/kg rapamycin intraperitoneally every other day (n = 5 mice) for 18 successive days as previous described [24]. Tumor growth was estimated by measuring the size of tumor. Tumor volumes were calculated every other day according to the formula (width2 × length)/2 as previous described [7-9]. The mice were euthanized at the 28th day by CO_2 inhalation and tumors were captured and embedded in paraffin for immunohistochemical staining or frozen at -80°C for Western blot analysis.

Immunohistochemistry, scoring system, hierarchical clustering and date visualization

Immunohistochemistry for serial cut of human tissue microarray (T12-412-TMA1) and nude mice xenograft specimen were performed as below described. All slides were rehydration and antigen retrieval using sodium citrate (pH = 6.0) in a pressure cooker except EGFR and p-Stat3^{T705} (EDTA buffer). Then the slides were treated in 3% hydrogen peroxide to block endogenous peroxidase activity and blocked with 2.5% bovine serum album in PBS buffer. Primary antibody were used with the following dilutions: p-S6$^{S235/236}$ (1:200), EGFR (1:200), p-Stat3^{T705} (1:200), HIF-1α (1:200), PAI (1:200), CD34 (1:200), Ki-67 (1:400). Slides were incubated at 4°C overnight with indicated primary antibody and incubated with biotin-labeled secondary antibody and streptavidin peroxidase consequently, visualized by diaminobenzidine and counterstaining with hematoxylin. The immunohistochemical staining was scanned using an Aperio ScanScope CS whole slice scanner (Vista, CA, USA) with background subtraction. The positive result was quantified using Aperio Quantification software for membrane, nuclear, or pixel quantification and histoscore were calculated using formula (3+) × 3 + (2+) × 2 + (1+) × 1 as previous described [24]. Immunohistochemical staining histoscore were converted into -3 to 3 using Microsoft Excel software as previously described. Cluster 3.0 with average linkage based on Pearson's correlation coefficient was used to achieve the hierarchical analysis and visualized via the Java TreeView1.0.5. [25].

Immunofluorescence histochemistry

SACC-83 cells plated on coverslip in 24 well palates and culture overnight and allowed to grown to 50% confluence. Cells were then treated with 100 nM rapamycin for 24 hours. After that, the cells were washed with PBS and fixed in 4% paraformaldehyde overnight at 4°C. They were permeabilized with 0.1% Triton X-100 for 10 min and blocked with bovine serum albumin (BSA) buffer for 1 hour. Cells were incubated with the anti-p-Stat3 antibody (1:100) overnight at 4°C, and treated with dyelight549 -labeled anti-rabbit antibody diluted 1:200 for 1 hour. The cells were then captured using a CLSM-310, Zeiss fluorescence microscope.

Statistical analysis

Data analysis was performed with GraphPad Prism 5.00 for Windows (GraphPad Software, Inc). The One-way ANOVA followed by the post-Tukey or Bonferroni multiple comparison tests was used to analyze the differences in immunostaining staining. The correlated expression of these markers was calculated by Two-tailed Pearson Statistics after confirmation of the sample with Gaussian distribution. Student t test were used to compare tumor burden between and immunohistochemical histoscore between vehicle and rapamycin treated group. All values were expressed as Mean values ± SEM. $P < 0.05$ were defined statistically significant.

Results

Immunohistochemical findings: high expression of p-S6$^{S235/236}$, EGFR, p-Stat3^{T705}, HIF-1α and PAI in human AdCC

As our previous data show that PI3K/AKT/mTOR activation in human AdCC are significantly increased as compared with adjacent normal salivary gland tissue. However, the role of mTOR for angiogenesis has remained unclear in human AdCC. To further elucidate the role of mTOR for angiogenesis, we assessed the expression of p-S6$^{S235/236}$ (a downstream target of mTOR), p-Stat3^{T705}, PAI, EGFR, and HIF-1α using human tissue microarray containing 72 AdCC, 12 PMA and 18 NSG. The representative IHC staining images for NSG, PMA and AdCC

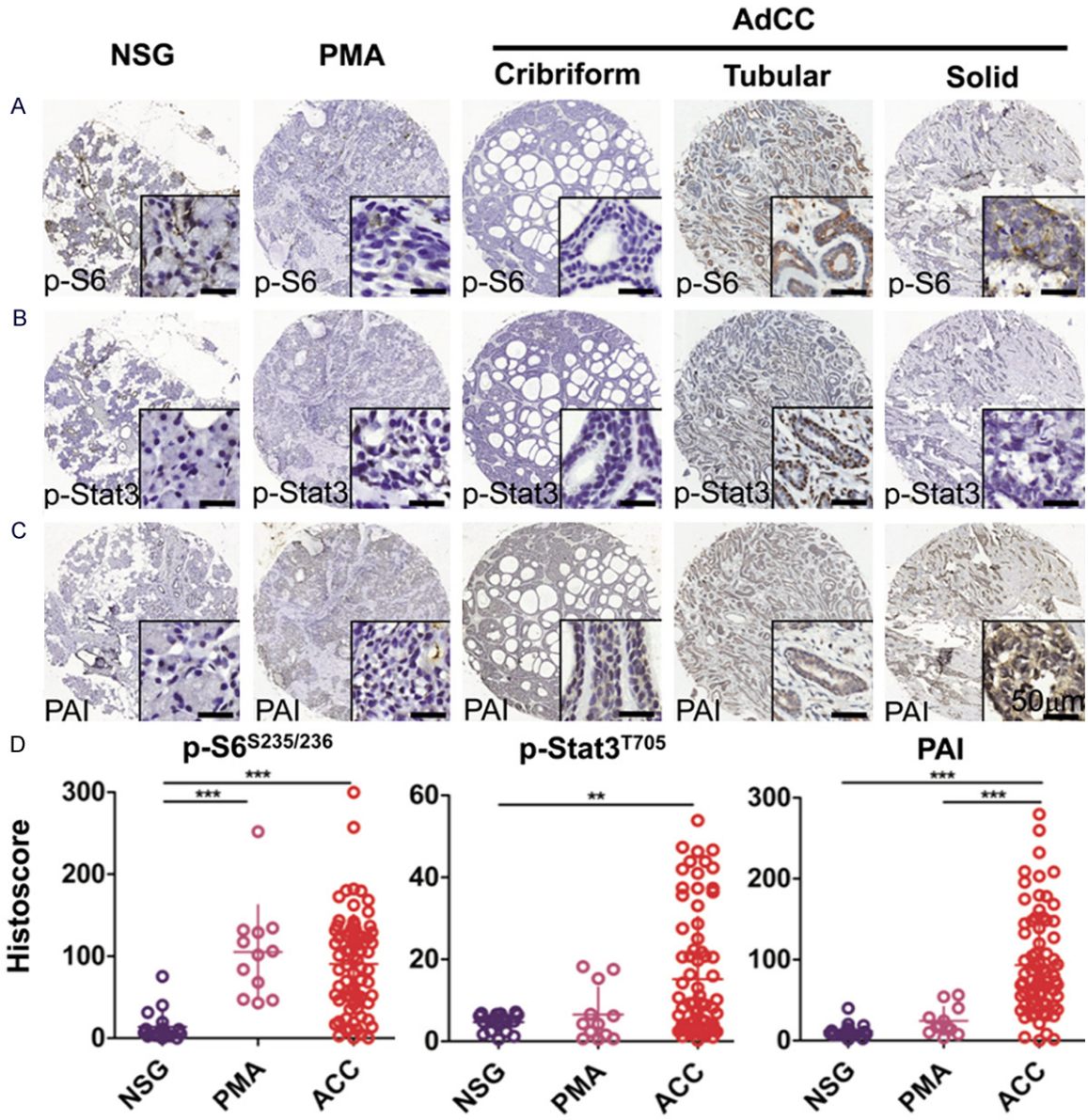

Figure 1. Analysis of tissue microarray cores for Immunohistochemistry Representative images from immunohistochemical staining of p-S6$^{S235/236}$ cytoplasmic and membrane expression. (A) p-Stat3^{T705} nuclear expression (B) PAI cytoplasmic and nuclear expression (C) in human normal salivary gland (NSG), polymorphism adenoma (PMA) and cribriform, tubular or solid type adenoid cystic carcinoma (AdCC). Scale bar = 50 μm. (D) Quantification of p-S6$^{S235/236}$, p-Stat3^{T705}, PAI expression levels in human NSG, PMA and AdCC tissue using AperioScanscope scanner and software. Data were analyzed by GraphPad Prism 5 software. (Mean ± SEM; $**p < 0.01$; $***p < 0.001$).

were shown in **Figure 1A** and Figure S1. We found that p-S6$^{S235/236}$ protein was slightly detected in cytoplasm and nuclear from NSG and weakly expressed in cytoplasm in PMA. Whereas, strong positive of p-S6$^{S235/236}$ was detected in cytoplasm from AdCC, especially in inner epithelial ductal cells of tubular pattern and irregular cancer nests of solid form (**Figure 1A**). The data is consistent with our previous finding. For EGFR, only slight expression was found in cytomembrane and cytoplasm from NSG and PMA, but obvious expression in cytomembrane and cytoplasm from AdCC (Figure S1A). Mildly expression of p-Stat3^{T705} in nuclear was inspected from NSG and PMA, but strongly expressed was tested from AdCC (**Figure 1B**). In NSG and PMA, HIF-1α was moderately stained in nuclear. In AdCC, HIF-1α was strongly stained

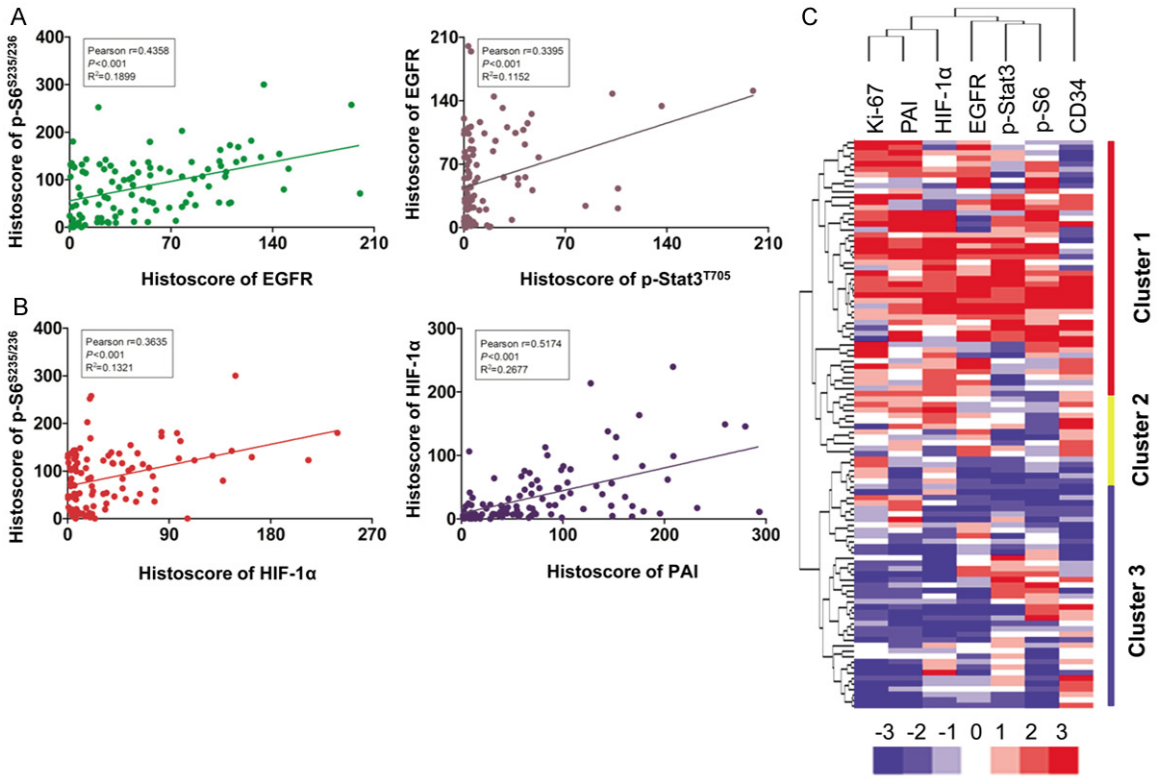

Figure 2. Correlation and regression of p-S6$^{S235/236}$ with EGFR, p-Stat3^{T705}, HIF-1α and PAI in human NSG, PMA and AdCC. A: The expression of p-S6$^{S235/236}$ had significant correlations with EGFR ($p < 0.001$, r = 0.4358, n = 102, left) and expression of EGFR had significant correlations with p-Stat3^{T705} ($p < 0.001$, r = 0.3395, n = 102, right) in human normal salivary gland (NSG), polymorphism adenoma (PMA) and adenoid cystic carcinoma (AdCC) by analyzing the tissue microarray immunohistochemical staining. B: The expression of p-S6$^{S235/236}$ had significant correlations with HIF-1α (P < 0.001, r = 0.3635, n = 102, left) and expression of HIF-1α had significant correlations with PAI ($p < 0.001$, r = 0.5174, n = 102, right) in human NSG, PMA and AdCC. Two-tailed Pearson test. C: Hierarchical clustering of immunohistochemical results of human AdCC with p-S6$^{S235/236}$, EGFR, p-Stat3^{T705}, HIF-1α, PAI, CD34 and Ki67 (Statistics including AdCC, NSG and PMA tissue).

in nuclear. In tubular type of AdCC, IHC staining was not only detected in nucleus but also in cytoplasm (Figure S1B). Moderate expression PAI, was inspected in nuclear from NSG and PMA. While strong positive was located in cytoplasm and nuclear from AdCC (**Figure 1C**).

Quantification of immunohistochemical staining

To credibly illustrate high expression of p-S6$^{S235/236}$, EGFR, p-Stat3^{T705}, HIF-1α, PAI in human AdCC, we quantified the immunohistochemical stain of whole slide by Aperio ScanScope CS scanner (Vista, CA, USA). Nuclear analysis of p-Stat3^{T705}, HIF-1α and membrane analysis of EGFR, p-S6$^{S235/236}$ were calculated with Aperio nuclear count software (Version 1.0) and membrane count software (Version 1.0). Cytoplasm PAI expression was calculated using Aperio positive pixel count software (Version 9.1). We found that AdCC cells showed significant staining for p-S6$^{S235/236}$ as compared with NSG ($p < 0.001$). PMA cells also showed significant staining for p-S6$^{S235/236}$ as compared with NSG ($p < 0.001$). There was slightly increase of p-S6$^{S235/236}$ staining in AdCC as compared with PMA, while the difference was not reach a statistic significant ($p > 0.05$) (**Figure 1D**). For EGFR, AdCC cells showed significant staining as compared with PMA and NSG ($p < 0.05$, $p < 0.001$, respectively) (Figure S1C). For p-Stat3^{T705}, however, there was mildly increase in AdCC as compared with NSG to reach a statistic significant ($p < 0.01$, **Figure 1D**). HIF-1α and PAI was highly expressed in AdCC tissues as compared with PMA ($p < 0.01$ for HIF-1α and $p < 0.001$ for PAI respectively) and NSG ($p < 0.05$ for HIF-1α and $p < 0.001$ for PAI respectively) (**Figure 1D** and Figure S1D).

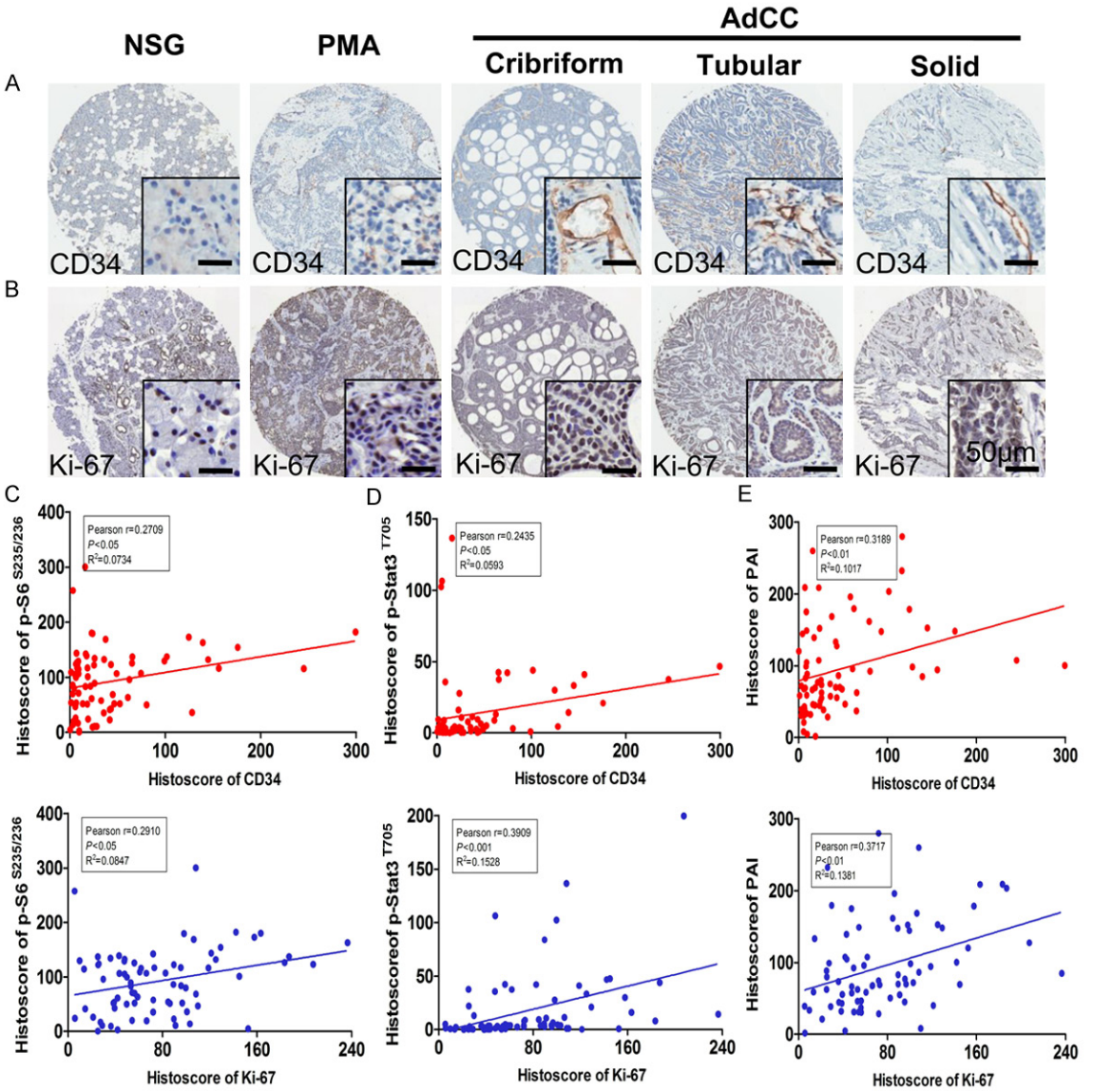

Figure 3. Overexpression of p-S6^{S235}, EGFR/p-Stat3^{T705}, HIF-1α/PAI correlated with CD34 and Ki67 in human AdCC tissue. Representative membranous staining of CD34 (A) and nuclear staining of Ki-67 (B) in human NSG, PMA and AdCC tissue samples. Scale bar = 50 μm. Correlation of p-S6$^{S235/236}$ (C), p-Stat3^{T705} (D) and PAI (E) with CD34 (upper) and Ki-67 (under) expression levels in human NSG, PMA and AdCC (n = 102). Two-tailed Pearson test.

Taken together, the expression of p-S6$^{S235/236}$, EGFR, p-Stat3^{T705}, HIF-1α and PAI was significantly increased in AdCC as compared with NSG as well as PA. To further determine whether the expression of p-S6$^{S235/236}$, EGFR, p-Stat3^{T705}, HIF-1α and PAI associates with histopathology pattern of AdCC, we analyzed these makers expression in cribriform, tubular and solid form of AdCC. While, the three patterns of AdCC have no statistics significance in p-S6$^{S235/236}$, EGFR, p-Stat3^{T705}, HIF-1α and PAI expression (Figure S1E).

The correlation between p-S6$^{S235/236}$ and EGFR/p-Stat3^{T705} and HIF-1α/PAI signaling pathway in human NSG, PMA and AdCC

To evaluate the association of mTOR/p-S6$^{S235/236}$ signaling pathway with EGFR/p-Stat3^{T705} and HIF-1α/PAI signaling pathway in human NSG, PMA and AdCC, we analyzed the quantative outcome of immunohistochemial staining by the Spearman rank correlation coefficient test and linear tendency test. The result demonstrates that activation of mTOR, which is indi-

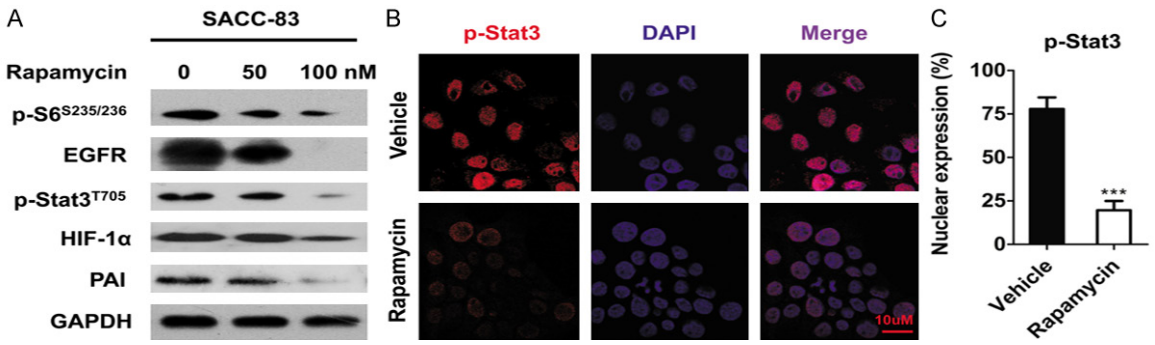

Figure 4. Rapamycin suppress p-S6$^{S235/236}$, EGFR, p-Stat3^{T705}, HIF-1α and PAI expression in SACC-83 cells. A: Western blot was performed for p-S6$^{S235/236}$, EGFR, p-Stat3^{T705}, HIF-1α and PAI expression in 0 nM, 50 nM and 100 nM rapamycin-treated SACC-83 cells. GAPDH was used as loading control. B: Immunofluorescence revealed inhibition of p-Stat3^{T705} nuclear expression in rapamycin-treated SACC-83 cells. C: Quantification of p-Stat3^{T705} nuclear expression by computer-assisted image analysis.

cated by high phosphorylation level of p-S6, correlated with over expression of EGFR (p < 0.001, r = 0.4358; **Figure 2A** left) as well as increase phosphorylation level of p-Stat^{T705} (p < 0.001, r = 0.3395; **Figure 2A** right). Similarly, increase phosphorylation of S6 correlated the expression of HIF-1α (p < 0.001, r = 0.3635; **Figure 2B** left) and increased nuclear expression of HIF-1α promotes the expression of PAI (p < 0.001, r = 0.5174; **Figure 2B** right). By clustering, these relationships in human AdCC was displayed in a visual image (**Figure 2C**), EGFR and p-Stat3^{T705} has closer correlation with p-S6$^{S235/236}$. Of interest, using hierarchical clustering analysis, most of the AdCC cases (cluster 1) were distinct from PMA (cluster 2) and NSG (cluster 3), reflecting the significant differences in p-S6$^{S235/236}$, EGFR, p-Stat3^{T705}, HIF-1α and PAI staining in AdCC.

Activation of mTOR promotes angiogenesis in human AdCC

To evaluation of the relationship between mTOR and angiogenesis, we performed IHC staining for CD34. We found that CD34 defined microvessels (< 100 μM) are notably detected in human AdCC as compared with NSG and PMA (**Figure 3A**). Relative higher expression of CD34 was statistically associated with over expression of p-S6$^{S235/236}$ (p < 0.05, r = 0.2709; **Figure 3C** upper), p-Stat3^{T705} (p < 0.05, r = 0.2435. **Figure 3D** upper) and PAI (p < 0.05, r = 0.3189; **Figure 3E** upper) using the Pearson correlation coefficient test. In addition, strong staining of Ki67 was detected in human AdCC as compared with NSG and PMA (**Figure 3B**). The expression of higher Ki67 was statistically associated with p-S6$^{S235/236}$ (p < 0.05, r = 0.2910; **Figure 3C** under), p-Stat3^{T705} (p < 0.001, r = 0.3909; **Figure 3D** under), and PAI (p < 0.01, r = 0.3717; **Figure 3E** under). These indicated an obvious positive correlation between mTOR-mediated EGFR/p-Stat3^{T705}, HIF-1α/PAI and angiogenesis as well as proliferation in human AdCC.

Rapamycin suppress the expression of p-S6$^{S235/236}$, EGFR, p-Stat3^{T705}, HIF-1α and PAI in human SACC-83 cell line

Base on the observation that expression of p-S6$^{S235/236}$ correlated with EGFR, p-Stat3^{T705}, HIF-1α and PAI staining in AdCC. To direct investigate the effect of mTOR inhibition on human AdCC cell line, we performed in vitro inhibition assay of rapamycin, a putative mTOR inhibitor on SACC-83 cell line. Western blot results revealed expression of p-S6$^{S235/236}$, EGFR, p-Stat3^{T705}, HIF-1α and PAI were significantly suppressed when SACC-83 cells were treated with 50 and 100 nM Rapamycin as compared with vehicle group (**Figure 4A**). Immunofluorescence revealed that rapamycin significantly decrease p-Stat3^{T705} nuclear expression (**Figure 4B** with quantification in **Figure 4C**).

Inhibition of mTOR attenuate growth of SACC-83 cell xenograft tumor by decreasing EGFR/p-Stat3^{T705} and HIF-1α/PAI in nude mice

To further confirm the mechanisms that mTOR regulates tumor angiogenesis, we established

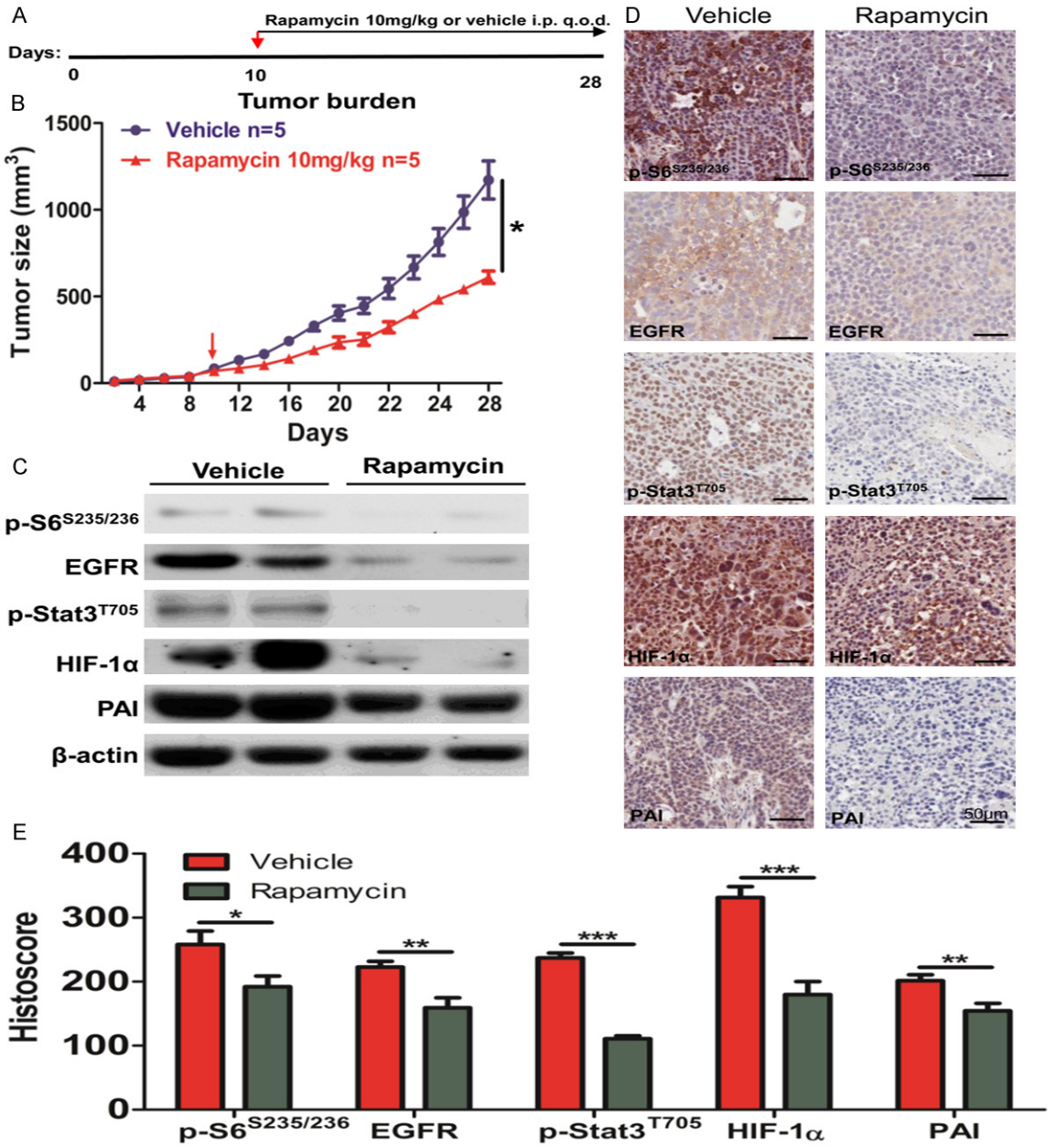

Figure 5. mTOR inhibition by rapamycin inhibit growth of SACC-83 cell xenograft tumor. A: Schematic graph shows drug delivery strategy of rapamycin or vehicle application in tumorigenesis experiment of SACC-83 nude mice xenograft. B: Rapamycin treatment significantly ($p < 0.05$) reduced tumor burden of SACC-83 nude mice xenograft as compared with vehicle group: (n = 5 respectively). Red arrow depicts the start of treatment when xenograft tumor visible. $^{*}p < 0.05$: student t test at 28 days. C: Western bolt analysis of the expression of p-S6$^{S235/236}$, EGFR, p-Stat3^{T705}, HIF-1α and PAI in vehicle and rapamycin treatment group. GADPH was used as loading control. D: Representative xenograft histopathology photos of p-S6$^{S235/236}$, EGFR, p-Stat3^{T705}, HIF-1α and PAI immunohistochemical staining in vehicle and rapamycin treatment SACC-83 cells xenografts. E: Quantification the expression of p-S6$^{S235/236}$, EGFR, p-Stat3^{T705}, HIF-1α and PAI using AperioScanscope and GraphPad Prism 5 software. (Scale bar = 50 μm. Mean ± SEM; $^{*}p < 0.05$; $^{**}p < 0.01$; $^{***}p < 0.001$).

SACC-83 nude mice xenograft to assess mTOR-mediated downstream pathway, including EGFR/p-Stat3^{T705}, HIF-1α/PAI. When tumors reached a palpable size, mice were treated with rapamycin (an inhibitor for mTOR) or vehicle for 18 successive days (**Figure 5A**). In rapamycin treatment group, rapamycin could significantly inhibit tumor growth ($p < 0.05$; **Figure 5B**). By

Western blot, we found p-S6$^{S235/236}$, EGFR, p-Stat3^{T705}, HIF-1α and PAI expression was down-regulation in rapamycin treated group as compared with vehicle group (**Figure 5C**). The result is further confirmed by immunohistochemistry, which shown p-S6$^{S235/236}$, EGFR, p-Stat3^{T705}, HIF-1α and PAI expression was down-regulation in rapamycin treated group xenograft tumor as compared with that in vehicle only group (**Figure 5D**). Analysis of the IHC staining histoscore, we confirmed rapamycin could inhibit EGFR/p-Stat3^{T705} and HIF-1α/PAI signaling pathway again (**Figure 5E**). All of the results are consistent with the findings in human AdCC.

Discussion

Our previous data suggested mTOR signaling pathway is a key and commonly dysregulated pathway in the progression of human salivary gland AdCC [6, 7]. In the present study, we investigate potential correlation of EGFR/p-Stat3^{T705} and HIF-1α/PAI pathway to reveal mechanisms on mTOR related angiogenesis. We initially found that p-S6$^{S235/236}$, EGFR, p-Stat3^{T705}, HIF-1α, PAI were highly expressed in AdCC as compared with PMA or NSG. Moreover, p-S6$^{S235/236}$-mediated EGFR/p-Stat3^{T705}, HIF-1α/PAI associated with CD34 and Ki67 to suggest high expression of p-S6$^{S235/236}$ promotes tumor angiogenesis and proliferaton by interact with EGFR/p-Stat3^{T705} and HIF-1α/PAI signaling pathway in human AdCC. Furthermore, in vitro and in vivo experiment direct observed that mTOR inhibition decrease expression of EGFR, p-Stat3^{T705}, HIF-1α, PAI as compared with vehicle group in SACC-83.

Stat3 is believed to be one of the mechanism in increasing tumor cell proliferation while blocking apoptosis in AdCC, which may IL6/JAK dependent or EGFR dependent [26]. EGFR has been proved to be an important Stat3-related factor in many solid tumors [18]. Inhibition of EGFR signaling significantly decrease AdCC cell line proliferation and epithelial mesenchymal transition [27]. In this study, we found the close relation of p-S6, EGFR and phosphorylation status of Stat3 with AdCC angiogenesis. In addition, we not only confirm the close relation of p-S6$^{S235/236}$ and EGFR/Stat3^{T705} in AdCC but also confirm that inhibition of mTOR may decrease the expression of EGFR and phosphorylation of Stat3. The accumulation of extracellular matrix (ECM), including laminin, fibronection and IV collagen, plays an important role in cancer development including AdCC [28]. The expression of PAI is able to prevent ECM degrading by banding uPA in AdCC cells [29]. ECM affects cancer progression by directly promoting cellular transformation, metastasis and facilitate tumor associated angiogenesis [30]. Hypoxia is a rather a common phenomenon in cancer. Under hypoxia circumstance, cancer cells usually acquire energy from glycolysis rather than oxidative phosphorylation. Hypoxia leads to a mass accumulation of pyruvate, the end-product glycolysis [31], which could promote tumor associated angiogenesis through PAI expression [31, 32]. By tissue array immunohistochemical staining analysis, we also observe that the high expression of HIF-1α and PAI have close relation with angiogenesis (CD34).

Up to now, rapamycin or its homologs were testified to be a potent therapeutic agent for some such highly malignant disease as acute lymphoblastic leukemia, hepatocellular carcinoma, cervical carcinoma, breast cancer and so on [33-36]. Molecular mechanism study indicate that rapamycin act on mTORC1 rather than mTORC2 to inhibit mTOR signaling pathway [37]. Our vivo study revealed that tumor growth was markedly inhibited in nude mice with rapamycin injection. Inhibition of AdCC growth through down-regulation of EGFR/p-Stat3^{T705} and HIF-1α/PAI signaling pathway [18, 31].

The expression of p-S6$^{S235/236}$, EGFR, p-Stat3^{T705}, HIF-1α and PAI is not only important to the tumorigenesis of AdCC but also has a diagnostic significance. All the five markers are highly expressed in AdCC as compared with NSG. To be honest, this study still has limitations because the cases of normal salivary gland and benign tumor are not large in number, and it is hard to cover all the features of the specimen and histological type. We further investigate the role of these markers in the differential diagnosis of the pathological type of AdCC because several studies have identified pathological factors in AdCC with an unfavorable effect on survival. However, our present data shows the expression of p-S6$^{S235/236}$, EGFR, p-Stat3^{T705}, HIF-1α and PAI did not reach statistical significance in three pathological type of AdCC.

Radiotherapy and chemotherapy remain as a primary treatment modality for human AdCC except most fundamental surgical resection. However, radiation usually has some side effects on gene expression by translational regulate [38]. The evaluation of radiation-induced gene expression revealed a number of genes and signaling networks that are involved in tumor genesis and progression [39]. It hinted that translation regulate may afford some target for radiosensitization to enhance treatment effect. Such as, hypoxia plays a irreplaceable role in radiation resistance due to a lack of in fixation of DNA damage [40]. Inhibition of HIF pathway could improve radiosensitivity and enhance local tumour control [41]. In our study, rapamycin were able to decrease the expression of HIF-1α in mice xenograft. But, whether rapamycin contributes to the improved outcome of radiotherapy in human salivary gland AdCC warrants further investigation.

In summary, our results revealed that p-$S6^{S235/236}$-mediated EGFR/p-$Stat3^{T705}$ and HIF-1α/PAI promotes AdCC angiogenesis and proliferation. Targeting mTOR by rapamycin can effectively reduce tumor growth and decrease the expression of p-$S6^{S235/236}$, EGFR, p-$Stat3^{T705}$, HIF-1α and PAI in AdCC cell line as well as xenograft tumor. It suggested that mTOR inhibitors may be a potential candidate for treatment of AdCC.

Acknowledgements

This work was supported by National Natural Science Foundation of China (81072203, 81272963, 81472528) to Z.J. Sun, (81371106) to L. Zhang, (81272946, 81472529) to W.F. Zhang and (81170977) to Y.F. Zhao. This work was also supported by program for new century excellent talents in university (NCET-13-0439), Ministry of Education of China to Z.J. Sun.

Disclosure of conflict of interest

The authors have declared that no competing interests exist.

Abbreviations

AdCC, adenoid cystic carcinoma; PMA, pleomorphic adenoma; NSG, normal salivary gland; mTOR, mammalian target of rapamycin; EGFR, epidermal growth factor receptor; Stat3, signal transducer and activator of transcription 3; HIFs, hypoxia induced factors; PAI, plasminogen activator inhibitor.

Address correspondence to: Zhi-Jun Sun or Lu Zhang, The State Key Laboratory Breeding Base of Basic Science of Stomatology & Key Laboratory of Oral Biomedicine Ministry of Education, Department of Oral and Maxillofacial-Head and Neck Oncology, School and Hospital of Stomatology, Wuhan University, Wuhan, China. Tel: 86-27-87686108; Fax: 86-27-87873260; E-mail: sunzj@whu.edu.cn (ZJS); luzhang2012@whu.edu.cn (LZ)

References

[1] Dincer N, Tezel GG, Sungur A, Himmetoglu C, Huebner K and Guler G. Study of FHIT and WWOX expression in mucoepidermoid carcinoma and adenoid cystic carcinoma of salivary gland. Oral Oncol 2010; 46: 195-199.

[2] Ellington CL, Goodman M, Kono SA, Grist W, Wadsworth T, Chen AY, Owonikoko T, Ramalingam S, Shin DM, Khuri FR, Beitler JJ and Saba NF. Adenoid cystic carcinoma of the head and neck: Incidence and survival trends based on 1973-2007 Surveillance, Epidemiology, and End Results data. Cancer 2012; 118: 4444-4451.

[3] Ho AS, Kannan K, Roy DM, Morris LG, Ganly I, Katabi N, Ramaswami D, Walsh LA, Eng S, Huse JT, Zhang J, Dolgalev I, Huberman K, Heguy A, Viale A, Drobnjak M, Leversha MA, Rice CE, Singh B, Iyer NG, Leemans CR, Bloemena E, Ferris RL, Seethala RR, Gross BE, Liang Y, Sinha R, Peng L, Raphael BJ, Turcan S, Gong Y, Schultz N, Kim S, Chiosea S, Shah JP, Sander C, Lee W and Chan TA. The mutational landscape of adenoid cystic carcinoma. Nat Genet 2013; 45: 791-798.

[4] Andry G, Hamoir M, Locati LD, Licitra L and Langendijk JA. Management of salivary gland tumors. Expert Rev Anticancer Ther 2012; 12: 1161-1168.

[5] Wang YF, Zhang W, He KF, Liu B, Zhang L, Zhang WF, Kulkarni AB, Zhao YF and Sun ZJ. Induction of autophagy-dependent cell death by the survivin suppressant YM155 in salivary adenoid cystic carcinoma. Apoptosis 2014; 19: 748-758.

[6] Chen G, Hu X, Zhang W, Xu N, Wang FQ, Jia J, Zhang WF, Sun ZJ and Zhao YF. Mammalian target of rapamycin regulates isoliquiritigenin-induced autophagic and apoptotic cell death in adenoid cystic carcinoma cells. Apoptosis 2012; 17: 90-101.

[7] Sun ZJ, Chen G, Zhang W, Hu X, Liu Y, Zhou Q, Zhu LX and Zhao YF. Curcumin dually inhibits both mammalian target of rapamycin and nu-

clear factor-kappaB pathways through a crossed phosphatidylinositol 3-kinase/Akt/IkappaB kinase complex signaling axis in adenoid cystic carcinoma. Mol Pharmacol 2011; 79: 106-118.

[8] Sun ZJ, Chen G, Zhang W, Hu X, Huang CF, Wang YF, Jia J and Zhao YF. Mammalian target of rapamycin pathway promotes tumor-induced angiogenesis in adenoid cystic carcinoma: its suppression by isoliquiritigenin through dual activation of c-Jun NH2-terminal kinase and inhibition of extracellular signal-regulated kinase. J Pharmacol Exp Ther 2010; 334: 500-512.

[9] Sun ZJ, Chen G, Hu X, Zhang W, Liu Y, Zhu LX, Zhou Q and Zhao YF. Activation of PI3K/Akt/IKK-alpha/NF-kappaB signaling pathway is required for the apoptosis-evasion in human salivary adenoid cystic carcinoma: its inhibition by quercetin. Apoptosis 2010; 15: 850-863.

[10] Molinolo AA, Amornphimoltham P, Squarize CH, Castilho RM, Patel V and Gutkind JS. Dysregulated molecular networks in head and neck carcinogenesis. Oral Oncol 2009; 45: 324-334.

[11] Shin S, Wolgamott L, Roux PP and Yoon SO. Casein Kinase 1ε promotes cell proliferation by regulating mRNA translation. Cancer Res 2014; 74: 201-11.

[12] Schindler C and Darnell JE Jr. Transcriptional responses to polypeptide ligands: the JAK-STAT pathway. Annu Rev Biochem 1995; 64: 621-651.

[13] Darnell JE Jr. STATs and gene regulation. Science 1997; 277: 1630-1635.

[14] Darnell JE Jr. Reflections on STAT3, STAT5, and STAT6 as fat STATs. Proc Natl Acad Sci U S A 1996; 93: 6221-6224.

[15] Garcia R, Bowman TL, Niu G, Yu H, Minton S, Muro-Cacho CA, Cox CE, Falcone R, Fairclough R, Parsons S, Laudano A, Gazit A, Levitzki A, Kraker A and Jove R. Constitutive activation of Stat3 by the Src and JAK tyrosine kinases participates in growth regulation of human breast carcinoma cells. Oncogene 2001; 20: 2499-2513.

[16] Fernandes A, Hamburger AW and Gerwin BI. ErbB-2 kinase is required for constitutive stat 3 activation in malignant human lung epithelial cells. Int J Cancer 1999; 83: 564-570.

[17] Kijima T, Niwa H, Steinman RA, Drenning SD, Gooding WE, Wentzel AL, Xi S and Grandis JR. STAT3 activation abrogates growth factor dependence and contributes to head and neck squamous cell carcinoma tumor growth in vivo. Cell Growth Differ 2002; 13: 355-362.

[18] Sato K, Nagao T, Iwasaki T, Nishihira Y and Fukami Y. Src-dependent phosphorylation of the EGF receptor Tyr-845 mediates Stat-p21waf1 pathway in A431 cells. Genes Cells 2003; 8: 995-1003.

[19] Vassalli JD, Sappino AP and Belin D. The plasminogen activator/plasmin system. J Clin Invest 1991; 88: 1067-1072.

[20] Gomes-Giacoia E, Miyake M, Goodison S and Rosser CJ. Targeting plasminogen activator inhibitor-1 inhibits angiogenesis and tumor growth in a human cancer xenograft model. Mol Cancer Ther 2013; 12: 2697-2708.

[21] Kimura H, Li X, Torii K, Okada T, Kamiyama K, Mikami D, Kasuno K, Takahashi N and Yoshida H. Glucocorticoid enhances hypoxia- and/or transforming growth factor-beta-induced plasminogen activator inhibitor-1 production in human proximal renal tubular cells. Clin Exp Nephrol 2011; 15: 34-40.

[22] Ueno M, Maeno T, Nomura M, Aoyagi-Ikeda K, Matsui H, Hara K, Tanaka T, Iso T, Suga T and Kurabayashi M. Hypoxia-inducible factor-1alpha mediates TGF-beta-induced PAI-1 production in alveolar macrophages in pulmonary fibrosis. Am J Physiol Lung Cell Mol Physiol 2011; 300: L740-752.

[23] Thompson L. World Health Organization classification of tumours: pathology and genetics of head and neck tumours. Ear Nose Throat J 2006; 85: 74.

[24] Sun ZJ, Zhang L, Hall B, Bian Y, Gutkind JS and Kulkarni AB. Chemopreventive and chemotherapeutic actions of mTOR inhibitor in genetically defined head and neck squamous cell carcinoma mouse model. Clin Cancer Res 2012; 18: 5304-5313.

[25] Eisen MB, Spellman PT, Brown PO and Botstein D. Cluster analysis and display of genome-wide expression patterns. Proc Natl Acad Sci U S A 1998; 95: 14863-14868.

[26] de Araujo VC, Furuse C, Cury PR, Altemani A and de Araujo NS. STAT3 expression in salivary gland tumours. Oral Oncol 2008; 44: 439-445.

[27] Huang Y, Yu T, Fu X, Chen J, Liu Y, Li C, Xia Y, Zhang Z and Li L. EGFR inhibition prevents in vitro tumor growth of salivary adenoid cystic carcinoma. BMC Cell Biol 2013; 14: 13.

[28] Shirasuna K, Watatani K, Furusawa H, Saka M, Morioka S, Yoshioka H and Matsuya T. Biological characterization of pseudocyst-forming cell lines from human adenoid cystic carcinomas of minor salivary gland origin. Cancer Res 1990; 50: 4139-4145.

[29] Shirasuna K, Saka M, Hayashido Y, Yoshioka H, Sugiura T and Matsuya T. Extracellular matrix production and degradation by adenoid cystic carcinoma cells: participation of plasminogen activator and its inhibitor in matrix degradation. Cancer Res 1993; 53: 147-152.

[30] Lu P, Weaver VM and Werb Z. The extracellular matrix: a dynamic niche in cancer progression. J Cell Biol 2012; 196: 395-406.
[31] Jung SY, Song HS, Park SY, Chung SH and Kim YJ. Pyruvate promotes tumor angiogenesis through HIF-1-dependent PAI-1 expression. Int J Oncol 2011; 38: 571-576.
[32] Dimova EY and Kietzmann T. The MAPK pathway and HIF-1 are involved in the induction of the human PAI-1 gene expression by insulin in the human hepatoma cell line HepG2. Ann N Y Acad Sci 2006; 1090: 355-367.
[33] Barrett D, Brown VI, Grupp SA and Teachey DT. Targeting the PI3K/AKT/mTOR signaling axis in children with hematologic malignancies. Paediatr Drugs 2012; 14: 299-316.
[34] Geng J, Li X, Lang X, Qiao C, Hu M, Yang J, Feng J and Lv M. Combination of Cetuximab and Rapamycin Enhances the Therapeutic Efficacy in Hepatocellular Carcinoma. Technol Cancer Res Treat 2013; 13: 377-85.
[35] Ueno S, Sudo T, Oka N, Wakahashi S, Yamaguchi S, Fujiwara K, Mikami Y and Nishimura R. Absence of human papillomavirus infection and activation of PI3K-AKT pathway in cervical clear cell carcinoma. Int J Gynecol Cancer 2013; 23: 1084-1091.
[36] Guilbert C, Annis MG, Dong Z, Siegel PM, Miller WH Jr. and Mann KK. Arsenic Trioxide Overcomes Rapamycin-Induced Feedback Activation of AKT and ERK Signaling to Enhance the Anti-Tumor Effects in Breast Cancer. PLoS One 2013; 8: e85995.
[37] Alayev A, Sun Y, Snyder RB, Berger SM, Yu JJ and Holz MK. Resveratrol prevents rapamycin-induced upregulation of autophagy and selectively induces apoptosis in TSC2-deficient cells. Cell Cycle 2013; 13: 371-82.
[38] Lu X, de la Pena L, Barker C, Camphausen K and Tofilon PJ. Radiation-induced changes in gene expression involve recruitment of existing messenger RNAs to and away from polysomes. Cancer Res 2006; 66: 1052-1061.
[39] Kumaraswamy S, Chinnaiyan P, Shankavaram UT, Lu X, Camphausen K and Tofilon PJ. Radiation-induced gene translation profiles reveal tumor type and cancer-specific components. Cancer Res 2008; 68: 3819-3826.
[40] Baumann M, Krause M and Hill R. Exploring the role of cancer stem cells in radioresistance. Nat Rev Cancer 2008; 8: 545-554.
[41] Helbig L, Koi L, Bruchner K, Gurtner K, Hess-Stumpp H, Unterschemmann K, Pruschy M, Baumann M, Yaromina A and Zips D. Hypoxia-inducible factor pathway inhibition resolves tumor hypoxia and improves local tumor control after single-dose irradiation. Int J Radiat Oncol Biol Phys 2014; 88: 159-166.

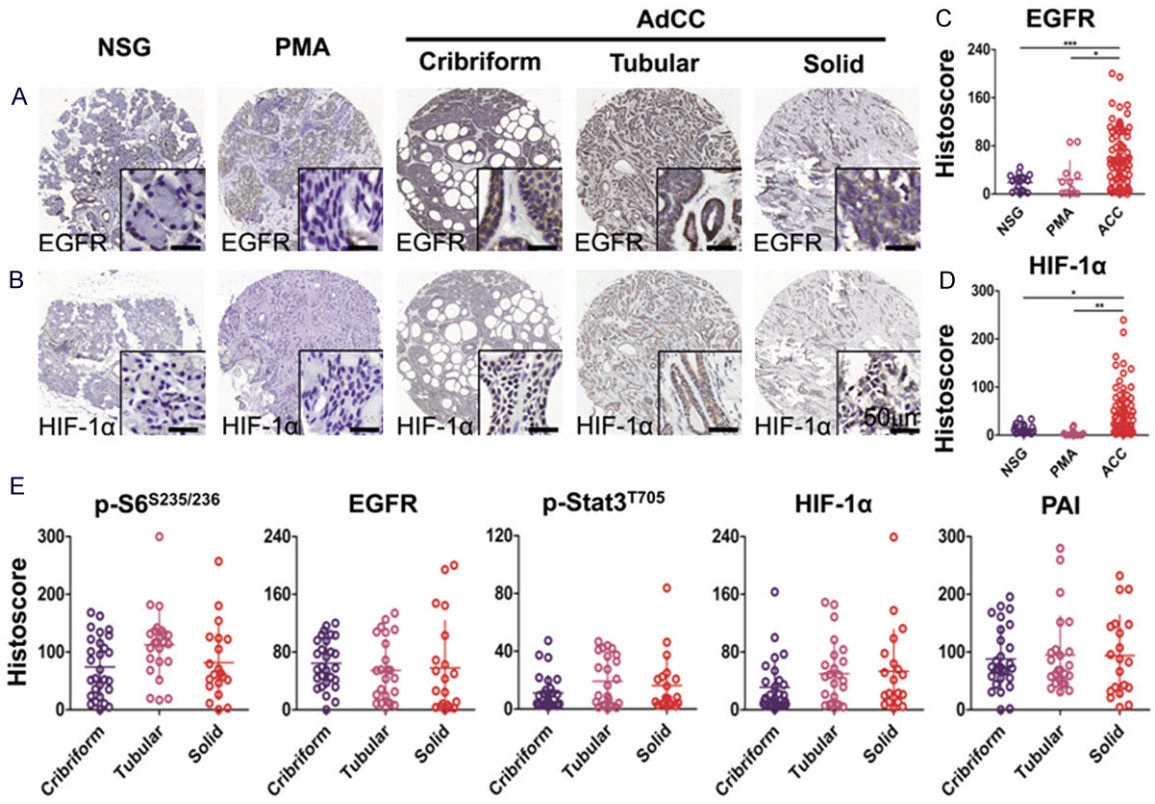

Figure S1. Immunohistochemical expression of EGFR and HIF-1α in human NSG, PMA and AdCC. Representative photos from immunohistochemical staining of EGFR membranous expression (A), HIF-1α cytoplasmic and nuclear expression (B) in human normal salivary gland (NSG), polymorphism adenoma (PMA) and cribriform, tubular or solid type adenoid cystic carcinoma (AdCC). Scale bar = 50 μm. Quantification of EGFR (C) and HIF-1α (D) expression levels in human NSG, PMA and AdCC tissue using Aperio Scanscope scanner and software. Data were analyzed by GraphPad Prism 5 software. (E) Quantification of p-S6$^{S235/236}$, EGFR, p-Stat3^{T705}, HIF-1α, PAI protein expression levels in pathology classfication of AdCC. (Mean ± SEM; $^{*}p < 0.05$; $^{**}p < 0.01$; $^{***}p < 0.001$).